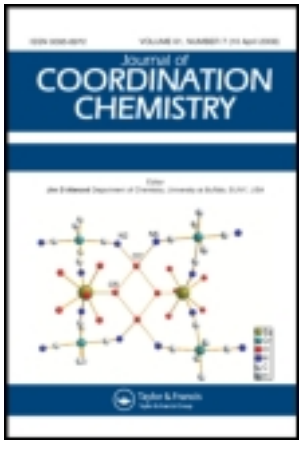

Journal of Coordination Chemistry
Publication details, including instructions for authors and subscription information:
http://www.tandfonline.com/loi/gcoo20

A novel Anderson-type polyoxometalate: hydrothermal synthesis, crystal structure, and catalytic performance of $(H_3O)[(3\text{-}C_5H_7N_2)_2(Cr(OH)_6Mo_6O_{18})]\cdot 3H_2O$

Zhen-Shan Peng [a], Chuan-Lei Zhang [a], Xiao-Ming Shen [a], Qian Deng [a] & Tie-Jun Cai [a]

[a] Key Laboratory of Theoretical Chemistry and Molecular Simulation of Ministry of Education, Hunan University of Science and Technology, Xiangtan 411201, China

Published online: 12 Aug 2011.

To cite this article: Zhen-Shan Peng, Chuan-Lei Zhang, Xiao-Ming Shen, Qian Deng & Tie-Jun Cai (2011) A novel Anderson-type polyoxometalate: hydrothermal synthesis, crystal structure, and catalytic performance of $(H_3O)[(3\text{-}C_5H_7N_2)_2(Cr(OH)_6Mo_6O_{18})]\cdot 3H_2O$, Journal of Coordination Chemistry, 64:16, 2848-2858, DOI: 10.1080/00958972.2011.607897

To link to this article: http://dx.doi.org/10.1080/00958972.2011.607897

Journal of Coordination Chemistry
Vol. 64, No. 16, 20 August 2011, 2848–2858

A novel Anderson-type polyoxometalate: hydrothermal synthesis, crystal structure, and catalytic performance of $(H_3O)[(3\text{-}C_5H_7N_2)_2(Cr(OH)_6Mo_6O_{18})]\cdot 3H_2O$

ZHEN-SHAN PENG, CHUAN-LEI ZHANG, XIAO-MING SHEN, QIAN DENG and TIE-JUN CAI*

Key Laboratory of Theoretical Chemistry and Molecular Simulation of Ministry of Education, Hunan University of Science and Technology, Xiangtan 411201, China

(*Received 10 April 2011; in final form 28 June 2011*)

A new Anderson polyoxometalate $(H_3O)[(3\text{-}C_5H_7N_2)_2(Cr(OH)_6Mo_6O_{18})]\cdot 3H_2O$ (3-$C_5H_6N_2$ = 3-aminopyridine) was hydrothermally synthesized and structurally characterized by single-crystal X-ray diffraction. Crystal data: triclinic, $P\bar{1}$, $a = 7.8482(8)$ Å, $b = 10.1800(10)$ Å, $c = 10.4103(10)$ Å, $\alpha = 88.031(3)^\circ$, $\beta = 78.308(2)^\circ$, $\gamma = 88.842(3)^\circ$, $V = 813.91$ Å^3, $Z = 1$, $R(F) = 0.0397$, $wR_{ref}(F^2) = 0.1022$, and $S = 1.076$. The X-ray crystallographic study showed that the structure contains Anderson-type $[Cr(OH)_6Mo_6O_{18}]^{3-}$ polyoxoanions. The title compound has high catalytic activity for the oxidation of acetone tested in a continuous-flow fixed-bed micro-reactor. When the initial concentration is 18.3 g m^{-3} in air and the flow velocity is 8.5 mL min^{-1}, the acetone is completely eliminated at 160°C.

Keywords: Polyoxometalate; Hydrothermal synthesis; Anderson type; Crystal structure; Acetone oxidation; Catalytic elimination

1. Introduction

Polyoxometalates (POMs) have applications in catalysis, medicine, and material sciences [1–4], owing to their unique structures and properties. Much attention has been paid to the design and synthesis of organic–inorganic hybrids through modification of metal oxides by organic molecules, leading to new materials [5]. A number of hybrid materials constructed of well-defined polyoxoanions, such as Keggin [6, 7], Wells–Dawson [8, 9], and Lindquist types [10, 11], have been reported. In La-Sheng Long's group, three Keggin-based supramolecular architectures, $Ni_2(Hbpy)_4(bpy)(H_2O)_6](SiW_{12}O_{40})_2\cdot 16H_2O$ (bpy = 4,4′-bipyridine), $[Ni(Hbpy)_2(bpy)(H_2O)_2](SiW_{12}O_{40})\cdot 6H_2O$, and $[SiW_{11}O_{39}Ni(4,4'\text{-bpy})][Ni(4,4'\text{-Hbpy})_2(H_2O)_2]$, have been reported, showing that the pH of the reaction plays a key role in the structural control of self-assembled processes [6]. An efficient method to prepare the functional hybrid organic–inorganic Wells–Dawson-type POMs has been devised by Bareyt's team, using a high-yielding phase transfer procedure to prepare tin-substituted R2- and

*Corresponding author. Email: tjcai53@163.com

ISSN 0095-8972 print/ISSN 1029-0389 online © 2011 Taylor & Francis
DOI: 10.1080/00958972.2011.607897

R1-Wells–Dawson polyoxotungstates [8]. For Lindquist type, Maatta [10] synthesized a POM incorporating an organoimido ligand, $[(n\text{-Bu})_4N]_2[Mo_5O_{18}(MoNC_6H_4CH_3)]$, which is the first direct spectroscopic measurement of neutral nitrocarbene.

Among polyoxoanions, Anderson-type polyoxoanions have planar structures and have been extensively employed as inorganic building blocks in the construction of organic–inorganic hybrid compounds. Das [12, 13] reported two Anderson-type heteropolyanion-supported copper phenanthroline complexes, $[M(OH)_6Mo_6O_{18}\{Cu(phen)(H_2O)_2\}_2]$ and $[M(OH)_6Mo_6O_{18}\{Cu(phen)(H_2O)Cl\}_2]\cdot 5H_2O$ (M) Al^{3+}, Cr^{3+}), with charge complementarity. Zhang [14] isolated two organic–inorganic hybrid compounds, $(H_3O)[Cu(C_6NO_2H_4)(phen)]_2[Al(OH)_6Mo_6O_{18}]\cdot 5H_2O$ and $(H_3O)[Cu(C_6NO_2H_4)(phen)]_2[Cr(OH)_6Mo_6O_{18}]\cdot 5H_2O$, built up of Anderson-type polyoxoanions and copper coordination polymers with 1,10-phenanthroline and pyridine-4-carboxylate ligands. Organic–inorganic hybrid compounds formed from an Anderson type of polyanion can provide new materials.

The Chinese Industrial Standard TJ 36-79 [15] states that the maximum allowable concentrations of acetone are $0.4\,g\,m^{-3}$ in a working zone and $8\times10^{-4}\,g\,m^{-3}$ in residential atmosphere, respectively. Thus, the eliminating acetone is important for environmental protection.

Due to the fact that Mo (or W) of Anderson-type polyoxoanions have two terminal oxygens with high reactivity, they could be used as catalysts to eliminate gas-phase organic pollutants.

In this article, we isolate an organic–inorganic hybrid compound, $(H_3O)[(3\text{-}C_5H_7N_2)_2Cr(OH)_6Mo_6O_{18})]\cdot 3H_2O$ (**1**), built up of Anderson-type polyoxoanions and 3-amino-pyridine; extensive $\pi\cdots\pi$ interactions and hydrogen-bonding interactions form 3-D supramolecular structures. The oxidative elimination of acetone from air was used to evaluate the catalytic activity of **1**. Herein, the syntheses, crystal structures, and catalytic properties are reported.

2. Experimental

All chemicals (reagent grade) were purchased commercially and used without purification. The crystal structure was determined using a Bruker SMART Apex II CCD area detector single-crystal diffractometer. Elemental analyses (C, H, and N) were performed on a Perkin Elmer 2400 CHNS/O analyzer. The Cr and Mo contents were determined by a Shimadzu ICPS-7510 instrument. Infrared spectra were recorded on a Perkin Elmer FTIR-2000 spectrophotometer with KBr pellets from 400 to 4000 cm^{-1}. UV-Vis spectra were recorded on a Perkin Elmer Lambda-35 spectrophotometer in DMSO. TG–DTA analysis was carried out on a WCT-1D differential thermal balance (Beijing Optical Instrument Factory, China) in air with a heating rate of $10^{\circ}C\,min^{-1}$.

The products of the catalytic reaction were analyzed on line by a GC-9800 gas chromatograph (GC) equipped with a column packed with Porapak-Q and using a flame ionization detector.

2.1. *Hydrothermal synthesis*

A single crystal suitable for X-ray diffraction analysis was prepared by hydrothermal reaction. A mixture of $CrCl_3\cdot 6H_2O$ (0.0600 g, 2.3 mmol), $Na_2MoO_4\cdot 2H_2O$ (0.1200 g,

Table 1. Crystallographic and refinement data for **1**.

Empirical formula	$C_{10}H_{29}CrMo_6N_4O_{28}$
Formula weight	1281.01
Crystal size (mm^3)	$0.50 \times 0.36 \times 0.18$
Crystal system	Triclinic
Space group	$P\bar{1}$
Unit cell dimensions (Å, °)	
a	7.8482(8)
b	10.1800(10)
c	10.4103(10)
α	88.031(3)
β	78.308(2)
γ	88.842(3)
Volume ($Å^3$), Z	813.91(14), 1
Calculated density ($g\,cm^{-3}$)	2.614
Absorption coefficient (Mo-Kα) (cm^{-1})	3.1
$F(0\,0\,0)$	616
Limiting indices	$-8 \le h \le +9$, $-9 \le k \le +2$, $-12 \le l \le +12$
Reflections measured	4911
Independent reflections	2729
Parameters refined	213
A/B values for weighing scheme[b]	0.1138/9.9393
Goodness-of-fit on F^2	1.076
$R(F)/wR(F^2)$[a] [$I > 2\sigma(I)$]	0.0397/0.1022
$R(F)/wR(F^2)$[a] (all data)	0.0411/0.1032
$\Delta\rho$fin (max./min.), $e\,Å^{-3}$	1.593/−1.305

[a] $wR_2 = \Sigma w(F_o^2 - F_c^2)^2 / 2\Sigma w(F_o^2)^2]^{1/2}$.
[b] $w = [\sigma^2(F_o^2) + (AP)^2 + BP]^{-1}$, where $P = (F_o^2 + 2F_c^2)/3$.

0.50 mmol), MoO_3 (0.6000 g, 4.2 mmol), 3-aminopyridine (0.0282 g, 0.03 mmol), 1 : 1 sulfuric acid 0.5 mL, and H_2O (14 mL) was sealed in a 25-mL Teflon-lined bomb, heated at 170°C for 120 h, and then slowly cooled to room temperature (RT). By filtrating, washing with distilled water, and air-drying, purple block-like crystals were collected in 45% yield (based on $CrCl_3 \cdot 6H_2O$). Anal. Calcd (%): C, 9.38; H, 2.28; N, 4.37; Mo, 44.94; and Cr, 4.06. Found: C, 9.42; H, 2.05; N, 4.25; Mo, 45.65; and Cr, 4.21.

2.2. *X-ray crystallography*

Reflection intensities of **1** were collected at 296(2) K using a Bruker SMART Apex II CCD area detector single-crystal diffractometer with confocally monochromated Mo-Kα radiation ($\lambda = 0.71073$ Å), using the $\Psi/2\vartheta$ scan method. An absorption correction was applied using the SADABS [16]. The structure was solved with Directed Methods using SHELXS-97 [17] and refined by full-matrix least-squares on F^2 (SHELXL-97 [18]). All hydrogens were generated geometrically and all non-hydrogen atoms were refined with anisotropic displacement parameters and hydrogens with isotropic displacement parameters.

Crystallographic data of **1** are summarized in table 1. Selected bond distances and angles for **1** are provided in table 2. Selected hydrogen-bonding parameters for **1** are listed in table 3.

Table 2. Selected interatomic distances (Å) and angles (°) for **1**.

Mo(1)–O(1)	1.687(6)	O(4)–Mo(3)#1	1.988(6)
Mo(1)–O(7)	1.699(6)		
Mo(1)–O(2)	1.947(6)		
Mo(1)–O(3)	1.951(6)	O(12)–Mo(3)#1	2.260(5)
Mo(1)–O(10)	2.274(5)		
Mo(1)–O(11)	2.314(5)	N(1)–C(5)	1.332(14)
Mo(2)–O(9)	1.696(6)	N(1)–C(3)	1.326(12)
Mo(2)–O(8)	1.701(6)		
Mo(2)–O(3)	1.936(6)	N(2)–C(1)	1.353(12)
Mo(2)–O(4)	1.977(6)		
Mo(2)–O(10)	2.280(5)		
Mo(2)–O(12)	2.285(5)	C(1)–C(3)	1.390(12)
Mo(3)–O(6)	1.694(6)	C(1)–C(2)	1.398(13)
Mo(3)–O(5)	1.726(6)	C(2)–C(4)	1.372(15)
Mo(3)–O(2)	1.916(6)		
Mo(3)–O(4)#1	1.988(6)		
Mo(3)–O(12)#1	2.260(5)	C(4)–C(5)	1.383(16)
Mo(3)–O(11)	2.290(5)		
Cr(1)–O(12)#1	1.970(5)		
Cr(1)–O(12)	1.970(5)		
Cr(1)–O(11)#1	1.973(5)		
Cr(1)–O(11)	1.973(5)		
Cr(1)–O(10)	1.976(5)		
Cr(1)–O(10)#1	1.976(5)		
O(1)–Mo(1)–O(7)	106.5(3)	O(12)–Cr(1)–O(10)	84.0(2)
O(1)–Mo(1)–O(2)	97.8(3)	O(11)#1–Cr(1)–O(10)	96.0(2)
O(7)–Mo(1)–O(2)	101.2(3)	O(11)–Cr(1)–O(10)	84.0(2)
O(1)–Mo(1)–O(3)	101.3(3)	O(12)#1–Cr(1)–O(10)#1	84.0(2)
O(7)–Mo(1)–O(3)	95.3(3)	O(12)–Cr(1)–O(10)#1	96.0(2)
O(2)–Mo(1)–O(3)	150.0(2)	O(11)#1–Cr(1)–O(10)#1	84.0(2)
O(1)–Mo(1)–O(10)	92.1(3)	O(11)–Cr(1)–O(10)#1	96.0(2)
O(7)–Mo(1)–O(10)	159.6(3)	O(10)–Cr(1)–O(10)#1	180.0(3)
O(2)–Mo(1)–O(10)	84.1(2)		
O(3)–Mo(1)–O(10)	72.4(2)		
O(1)–Mo(1)–O(11)	160.0(3)		
O(7)–Mo(1)–O(11)	92.5(3)		
O(2)–Mo(1)–O(11)	71.9(2)		
O(3)–Mo(1)–O(11)	82.7(2)		
O(10)–Mo(1)–O(11)	70.29(18)		
O(9)–Mo(2)–O(8)	106.0(3)		
O(9)–Mo(2)–O(3)	101.6(3)		
O(8)–Mo(2)–O(3)	98.1(3)		
O(9)–Mo(2)–O(4)	96.1(3)		
O(8)–Mo(2)–O(4)	99.8(3)		
O(3)–Mo(2)–O(4)	150.2(2)		
O(9)–Mo(2)–O(10)	93.0(3)		
O(8)–Mo(2)–O(10)	160.3(3)		
O(3)–Mo(2)–O(10)	72.5(2)		
O(4)–Mo(2)–O(10)	82.8(2)		
O(9)–Mo(2)–O(12)	159.8(3)		
O(8)–Mo(2)–O(12)	91.7(3)		
O(3)–Mo(2)–O(12)	85.1(2)		
O(4)–Mo(2)–O(12)	70.8(2)		
O(10)–Mo(2)–O(12)	70.63(19)		
O(6)–Mo(3)–O(5)	106.2(3)		
O(6)–Mo(3)–O(2)	99.0(3)		
O(5)–Mo(3)–O(2)	101.5(3)		
O(6)–Mo(3)–O(4)#1	99.5(3)		
O(5)–Mo(3)–O(4)#1	95.8(3)		

(*Continued*)

Table 2. Continued.

O(2)–Mo(3)–O(4)#1	150.0(2)
O(6)–Mo(3)–O(12)#1	92.8(3)
O(5)–Mo(3)–O(12)#1	158.8(3)
O(2)–Mo(3)–O(12)#1	84.5(2)
O(4)#1–Mo(3)–O(12)#1	71.2(2)
O(6)–Mo(3)–O(11)	161.5(3)
O(5)–Mo(3)–O(11)	91.9(3)
O(2)–Mo(3)–O(11)	72.9(2)
O(4)#1–Mo(3)–O(11)	82.2(2)
O(12)#1–Mo(3)–O(11)	70.20(18)
O(12)#1–Cr(1)–O(12)	180.000(1)
O(12)#1–Cr(1)–O(11)#1	96.8(2)
O(12)–Cr(1)–O(11)#1	83.2(2)
O(12)#1–Cr(1)–O(11)	83.2(2)
O(12)–Cr(1)–O(11)	96.8(2)
O(11)#1–Cr(1)–O(11)	180.0
O(12)#1–Cr(1)–O(10)	96.0(2)

Symmetry transformations used to generate equivalent atoms: #1 $-x+1$, $-y+2$, $-z$.

Table 3. Selected hydrogen-bonding geometry (Å, °) for **1**.

Donor–H···Acceptor	D–H	H···A	D–A	D–H···A
N1–H1···O3#1	0.86	1.91	2.754	165
N2–H2A···O2#2	0.86	2.21	2.991	150
N2–H2B···O8	0.86	2.17	2.952	151
O10–H10···O1W#3	0.98	1.70	2.651	163
O11–H11···O5#4	0.98	1.82	2.768	163
O12–H12···O2W#5	0.98	1.64	2.613	173
C3–H3···O1#2	0.93	2.48	3.335	153
C5–H5···O6#6	0.93	2.34	3.219	158
O1W–H1WA···O9#7	0.85	2.49	2.914	112
O1W–H1WB···O7#8	0.86	2.21	2.902	138
O2W–H2WA···O6#9	0.84	2.57	3.006	114
O2W–H2WA···O8	0.84	2.39	3.190	159
O2W–H2WB···O5#8	0.87	2.37	2.914	121

#1, $-x$,$1-y$,$1-z$; #2, x, $-1+y$, z; #3, x, $1+y$, z; #4, $-x$, $2-y$, $-z$; #5, $1-x$, $1-y$, $-z$; #6, $-x$, $2-y$, $1-z$; #7, $1-x$, $1-y$, $1-z$; #8, $1+x$, $-1+y$, z; and #9, $1-x$, $2-y$, $-z$.

2.3. *Catalytic reaction for acetone elimination*

Catalytic oxidation of acetone was used as a model reaction to evaluate the catalytic performance of **1**. Catalytic reactions were carried out in a continuous-flow fixed-bed micro-reactor (figure 1). 0.20 g of **1** was loaded in the catalytic reaction tube (φ/8 mm; L/200 mm) as a catalyst.

A model of polluted air containing acetone was prepared by bubbling clean air into a container filled with an acetone solution and then diluting the air containing acetone with clean dry air. The initial acetone concentration of the simulative polluted air was controlled by changing the proportion of the bubbling and diluent gases. The reactant mixture was fed to the tube reactor at a flow rate of 8.5 mL min^{-1} and concentration of 18.3 g m^{-3}.

At different reaction temperatures, the rate for eliminating acetone were determined from RT to a temperature at which acetone was no longer detected in the effluent gases.

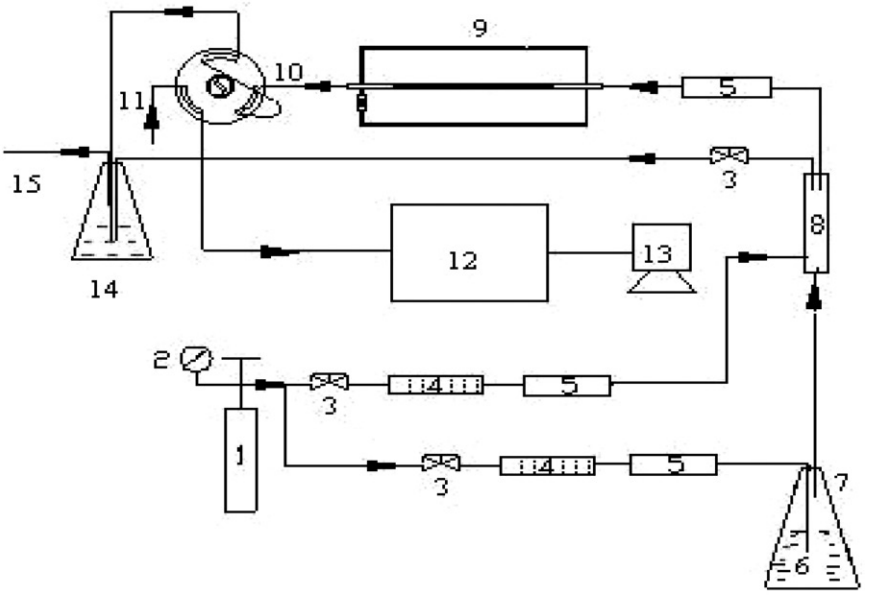

Figure 1. Continuous-flow reaction system. Air bottle, 2. Manometer, 3. Valve, 4. Desiccator, 5. Mass flow meter, 6. Acetone, 7. Container, 8. Gas mixed pipe, 9. Catalytic reactor, 10. Six-port valve, 11. Carrier gas, 12. GC, 13. GC work station, 14. Tail gas absorbing bottle, and 15. Put empty.

The concentrations of organic compounds in effluent gases were analyzed on line by a GC. The inorganic products of the effluent gases were monitored by a 0.2 (wt%) $PdCl_2$ solution and a saturated limewater solution. Blank experiments were carried out in the absence of **1**.

3. Results and discussion

Compound **1** was synthesized in aqueous solution. All Mo ions have charges +6 and Cr +3. Three protons are added to two 3-aminopyridines and a water for charge balance, similar to reported cases [19]. Compound **1** is formulated as $(H_3O)[(3\text{-}C_5H_7N_2)_2(Cr(OH)_6Mo_6O_{18})] \cdot 3H_2O$.

3.1. *Crystal structure description*

As shown in figure 2, **1** is built from one Anderson-type polyoxoanion, two protonated 3-aminopyridine cations, and four waters. The polyoxoanion $[Cr(OH)_6Mo_6O_{18}]^{3-}$ belongs to the B-type Anderson structure, consisting of seven edge-shared octahedra, six of which are Mo octahedra, arranged hexagonally around the central Cr. The Mo ions form approximately a regular planar hexagonal configuration circling the Cr. The molybdenum–oxygen bonds in **1** can be grouped into three sets: Mo–Ot (terminal oxygen), Mo–Ob (bridging oxygen), and Mo–Oc (central oxygen common to two

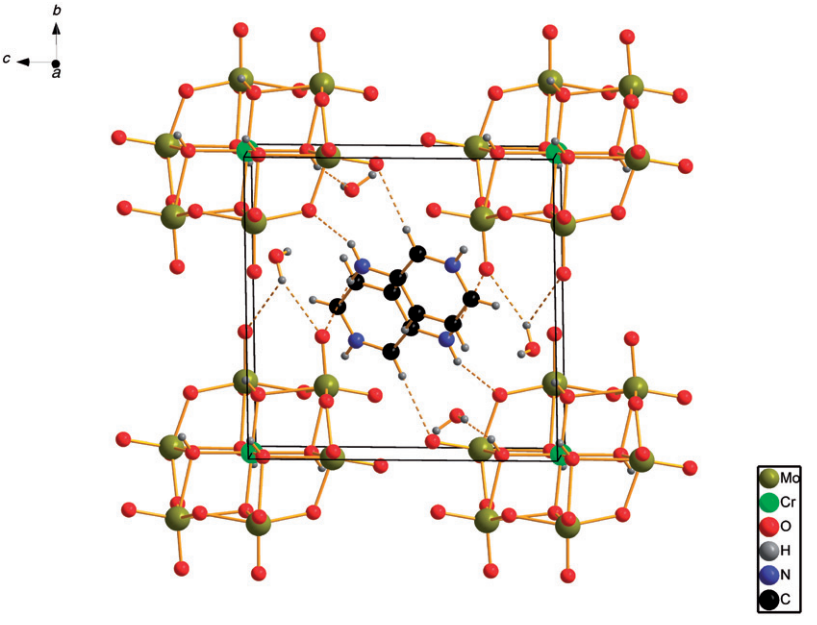

Figure 2. Packing diagram of **1** along the *a*-axis.

molybdenums and chromium). As summarized in table 2, the Cr–O distances range from 1.970(5) to 1.976(5) Å and the O–Cr–O bond angles from 83.20(2)° to 180.0(2)°. The Mo–O distances are from 1.690(5) to 2.310(4) Å, while the O–Mo–O bond angles from 70.36(13)° to 161.60(19)°. All bond lengths and angles are within normal ranges, consistent with those described [20].

There are many hydrogen bonds in the target crystal (table 3). The extensive hydrogen bonds involved with heteropolyanions, 3-aminopyridine, and water result in an intricate 2-D supramolecular network, as shown in figure 3.

Two 3-aminopyridines reside in the center of the unit cell, presenting a reverse parallel but no overlap. However, 3-aminopyridine in the unit cell and another 3-aminopyridine of the neighboring unit cell overlap, with $\pi\cdots\pi$ stacking interactions with the shortest C$\cdots$C distance of 3.572(6) Å. The supramolecular interactions endow **1** with an interesting 3-D supramolecular array.

3.2. *The characterization of 1*

The infrared spectra of **1** was tested before and after the catalytic reaction. For **1,** bands at 1643, 1613, 1567, and 1489 cm^{-1} are characteristic of pyridine and absorptions at 938, 916, 886, 793, and 655 cm^{-1} are ascribed to $[Cr(OH)_6Mo_6O_{18}]^{3-}$ [21]. The spectra taken before and after the catalytic reaction showed no change, indicating that **1** is stable under the catalytic reaction conditions.

The UV-Vis spectrum of an aqueous DMSO solution at RT is presented in figure 4. Strong ligand-to-metal charge transfer (LMCT) absorptions occur at 251 and 259 nm, which may be assigned to O$\rightarrow$Mo LMCT of $[Cr(OH)_6Mo_6O_{18}]^{3-}$ [22]. The weak

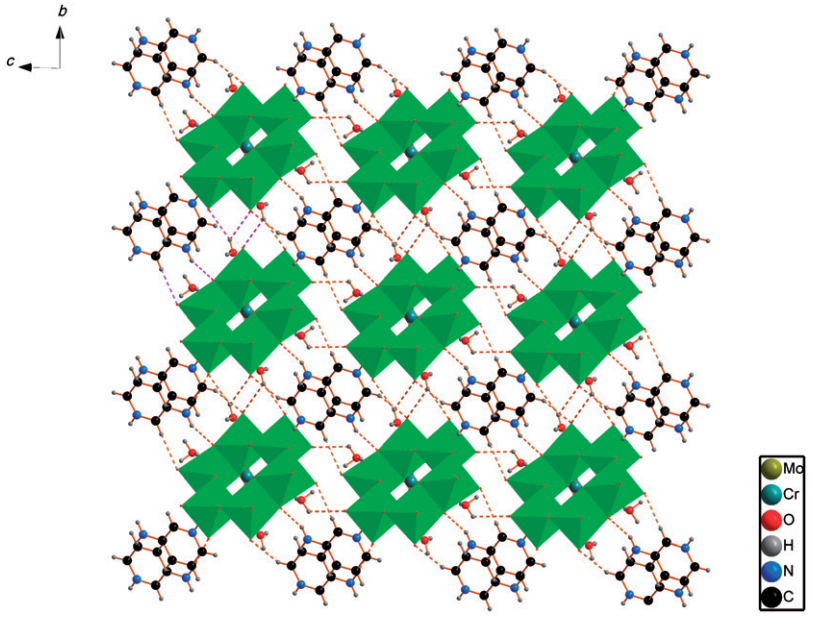

Figure 3. Polyhedral representation of the 2-D structure by hydrogen bonds along the *a*-axis in **1**.

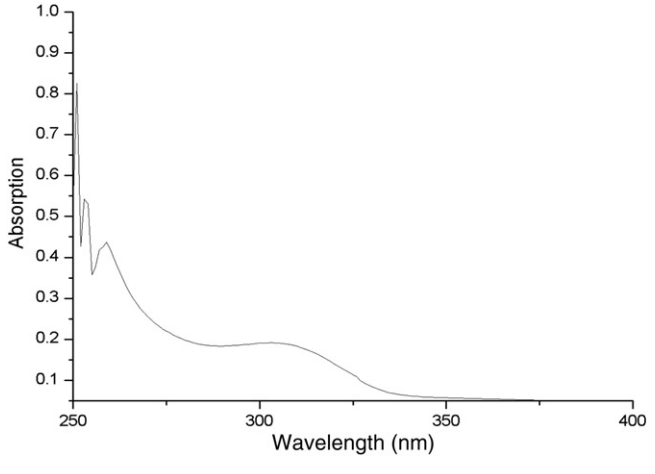

Figure 4. UV-Vis spectrum of **1** in aqueous DMSO.

absorption at 303 nm may indicate charge-transfer interactions between organic cations and polyoxoanions [23].

The TG–DTA curves of **1** exhibit two endothermic peaks and one exothermic peak at 129°C, 225°C, and 408°C, accompanying three weight losses, ascribed to the removal of water and decomposition of the organic molecules and polyanions. The TG curve of **1** shows a total weight loss of 25.92% at 90–500°C; the residues after TG–DTA may be

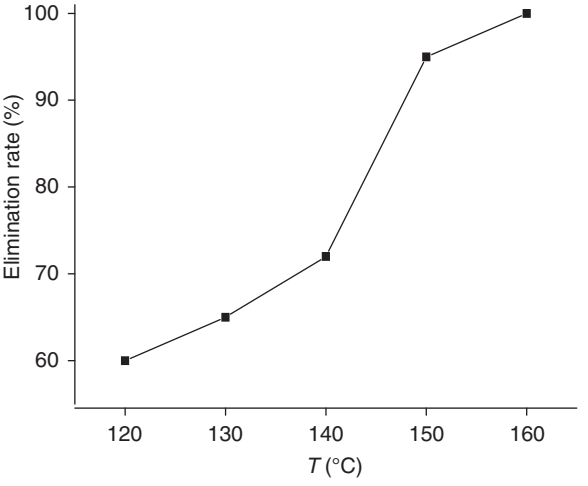

Figure 5. Curve of acetone elimination rate *vs.* temperature.

MoO_3 and Cr_2O_3, agreeing with the calculated value of 26.48%. The TG–DTA supports the chemical composition of **1**.

3.3. *Catalytic reaction*

Blank experiments show that acetone in a model of polluted air was not eliminated oxidatively without **1** as a catalyst. From the test results of the effluent gases after catalytic reaction, there is no new peak in the GC diagram, indicating no new organic compounds formed. The lime-saturated water showed precipitate, but the color of the 0.2% $PdCl_2$ solution did not change, indicating that there was CO_2 but no CO, suggesting CO_2 and H_2O as products.

The temperatures of the catalytic reactions were from 120°C to 160°C, lower than the decomposition temperature of **1**. The relationship between the elimination rate and temperature is shown in figure 5.

Compound **1** shows a high catalytic activity for oxidation of acetone tested in a continuous-flow fixed-bed micro-reactor. Acetone of concentration 18.3 g m^{-3} provided at a flow velocity 8.5 mL min^{-1} was completely eliminated at 160°C over 0.20 g of **1** as catalyst. This acetone concentration is much greater than the maximum concentration allowed by the national emission standards. Compound **1** has a better catalytic oxidation activity for eliminating acetone at lower temperature, providing experimental evidence for efficient catalysts under environmental governance.

4. Conclusions

We have synthesized a compound with 3-aminopyridine, Anderson-type polyoxoanion, and lattice water. Hydrogen bonds involved with heteropolyanions, 3-aminopyridine,

and water result in a 2-D network. The $\pi \cdots \pi$ stacking interactions are responsible for formation of the 3-D supramolecular array.

There were some Anderson-type complexes reported [12–14, 19] with structures based on Anderson-type polyoxoanions ($[M(OH)_6Mo_6O_{18}]^{3-}$, $M = Al^{3+}$, Cr^{3+}, Co^{3+}, etc.), organic molecule ($C_6H_{10}N_3O_2$, phen, bipy, etc.), and the transition metal cations (Cu^{2+}, Ag^{+}, Mn^{2+}, etc.) in which Anderson-type polyanions and organic molecules are ligands coordinating to the transition metal. Hydrogen bonds are responsible for supramolecular assembly, not π–π stacking interactions. Compound **1** is built up from Anderson-type polyanion, 3-aminpyridine, and water and no transition metal ions. The 3-aminopyridine does not coordinate to the metals, but π–π stacks, forming a supramolecule.

Compound **1** has a better catalytic oxidation activity for eliminating acetone at lower temperature. Acetone ($18.3\,g\,m^{-3}$) was completely eliminated at 160°C over 0.20 g of **1** as catalyst, within the national discharge standard concentration of acetone. Without any activation, **1** shows good catalytic activity, bringing out potential applications in catalytic oxidation.

Supplementary material

CCDC 781515 contains supplementary crystallographic data for this article. These data can be obtained free of charge from The Cambridge Crystallographic Data Centre *via* www.ccdc.cam.ac.uk/data request/cif

Acknowledgments

The project was supported by the Organic Chemistry Key Subject of Hunan Province and Key Laboratory of Theoretical Chemistry and the Molecular Simulation of Ministry of Education, Hunan University of Science and Technology.

References

[1] N. Mizuno, M. Misono. *Chem. Rev.*, **98**, 199 (1998).
[2] E. Coronado, C.J. Gomez-Garcia. *Chem. Rev.*, **98**, 273 (1998).
[3] A. Müller, F. Peter, M.T. Pope, D. Gatteschi. *Chem. Rev.*, **98**, 239 (1998).
[4] J.T. Rhule, C.L. Hill, D.A. Judd, R.F. Schinazi. *Chem. Rev.*, **98**, 327 (1998).
[5] L. Carlucci, G. Ciani, D.M. Proserpio. *Coord. Chem. Rev.*, **246**, 247 (2003).
[6] P.Q. Zheng, Y.P. Ren, L.S. Long, R.B. Huang, L.S. Zheng. *Inorg. Chem.*, **44**, 1190 (2005).
[7] Y.P. Ren, X.J. Kong, L.S. Long, R.B. Huang, L.S. Zheng. *Cryst. Growth Des.*, **6**, 572 (2006).
[8] S. Bareyt, S. Piligkos, B. Hasenknopf, P. Gouzerh, E. Lecôte, S. Thorimbert, M. Malacria. *J. Am. Chem. Soc.*, **127**, 6788 (2005).
[9] J.Y. Niu, D.J. Guo, J.P. Wang, J.W. Zhao. *Cryst. Growth Des.*, **4**, 241 (2004).
[10] Y. Du, A.L. Rheingold, E.A. Maatta. *J. Am. Chem. Soc.*, **114**, 345 (1992).
[11] Y.G. Wei, M. Lu, C.F.C. Cheung, C.L. Barnes, Z.H. Peng. *Inorg. Chem.*, **40**, 5489 (2001).
[12] V. Shivaiah, M. Nagaraju, S.K. Das. *Inorg. Chem.*, **42**, 6604 (2003).
[13] V. Shivaiah, S.K. Das. *Inorg. Chem.*, **44**, 8846 (2005).
[14] S.W. Zhang, Y. Li, Y. Liu, R. Cao, C.Y. Sun, H.M. Ji, S.X. Liu. *J. Mol. Struct.*, **920**, 284 (2009).

[15] States Environmental Protection Agency (SEPA). *Chemical's Toxicity, Law and Environmental Data Manual*, China Environmental Science Press, Beijing (1992).
[16] G.M. Sheldrick. *SADABS*, University of Göttingen, Göttingen, Germany (2002).
[17] G.M. Sheldrick. *SHELXS-97, Program for the Solution of Crystal Structures*, University of Göttingen, Göttingen, Germany (1997).
[18] G.M. Sheldrick. *SHELXL-97, Program for the Refinement of Crystal Structures*, University of Göttingen, Göttingen, Germany (1997).
[19] P.P. Zhang, J. Peng, A.X. Tian, H.J. Pang, Y. Chen, M. Zhu, D.D. Wang, M.G. Liu, Y.H. Wang. *J. Coord. Chem.*, **63**, 3610 (2010).
[20] R.G. Cao, S.X. Liu, Y. Liu, Q. Tang, L. Wang, L.H. Xie, Z.M. Su. *J. Solid State Chem.*, **182**, 49 (2009).
[21] R.G. Cao, S.X. Liu, L.H. Xie, Y.B. Pan, J.F. Cao, Y.H. Ren, L. Xu. *Inorg. Chem.*, **46**, 3541 (2007).
[22] Z.F. Li, R.R. Cui, B. Liu, G.L. Xue, H.M. Hu, F. Fu, J.W. Wang. *J. Mol. Struct.*, **920**, 436 (2009).
[23] Y.M. Xie, Q.S. Zhang, Z.G. Zhao, X.Y. Wu, S.C. Chen, C.Z. Lu. *Inorg. Chem.*, **47**, 8086 (2008).